PNAS
www.pnas.org

Supplementary Information for

FGF-2-dependent signaling activated in aged human skeletal muscle promotes intramuscular adipogenesis

Sebastian Mathes, Alexandra Fahrner, Umesh Ghoshdastider, Hannes A. Rüdiger, Michael Leunig, Christian Wolfrum, and Jan Krützfeldt

corresponding author: Jan Krützfeldt
Email: jan.kruetzfeldt@usz.ch

This PDF file includes:

Supplementary Materials and Methods

Patients. Biopsies from the Tensor fasciae latae muscle were obtained during elective hip replacement surgery in 11 patients between April 2019 and June 2020 at the Schulthess Clinic, Zurich, Switzerland. Inclusion criteria was age of at least 18 years and the pre-defined age limit of <55 years for the group "young" and >75 years for the group "aged". Exclusion criteria was a known HIV or hepatitis infection. The young group included 3 females and 2 males, age was 36.0 ± 7.2 years with body mass index (BMI) 25.7 ± 2.4 kg/m^2 (mean ± SEM). The aged group included 3 females and 3 males, age was 79.3 ± 1.6 years ($p \leq 0.001$, two-tailed unpaired Student´s t test compared to young) with BMI 25.8 ± 1.9kg/m^2 ($p = 0.994$).

Animals. All animals used were male mice housed at 3-5 littermates per cage in individually ventilated cages under conditions of controlled temperature (22 °C) and illumination (12-h light/12-h dark cycle; light off at 6 p.m.) with *ad libitum* access to chow and water. Health status of all mouse lines were monitored on a regular basis according to FELASA guidelines. *ACTA1*-cre/Esr1 mice (Jackson; No. 031934) were crossed with *miR29ab1*$^{fl/fl}$ mice (1) for the inducible skeletal muscle-specific ablation of miR-29a. Recombination of the floxed allele was induced by intraperitoneal injections of 2 mg tamoxifen (Sigma) for five consecutive days. *Pax7*-Cre mice (Jackson; No. 010530) were crossed to *miR29ab1*$^{fl/fl}$ mice for tissue-specific excision of the floxed segment in skeletal muscle satellite cells. Respective primers used for genotyping are listed in Supplemental Table 1. Wildtype C57BL/6J mice were obtained from Envigo (Horst, Netherlands). Aged (25 months) and young control (2 months) C57BL/6JRj mice were obtained from Janvier Labs (France). Aged C57BL/6JRj mice or 12 to 14-week old mice of the *miR29ab1*$^{fl/fl}$ mouse line maintained on a mixed C57BL/6J;129 genetic background were used for fatty infiltration experiments. Mice were anaesthetized with isofluorane (Forane) and carprofen (Rimadyl) s.c. and tibialis anterior muscles were injected with 1.5×10^{12} vg AAV in 50 µl PBS. Three weeks post-infection, IMAT formation was induced by intramuscular injection with 25 µl of 50% v/v glycerol (Sigma) in PBS and mice were sacrificed 2 weeks post-injection.

Cell preparation and FACS. Primary muscle cells from humans were obtained from our previously published study (2). Procedures for isolation of primary muscle cells from mouse skeletal muscle were performed as previously described (2). Skeletal muscle tissue was excised from the hind limbs. Muscles were minced and digested with 2 mg/mL collagenase type II (Gibco) in collagenase buffer (1.5% BSA in HBSS) for 1 h at 37 °C. Muscle slurries were filtered through a 100 µm cell strainer (BD Biosciences), followed by treatment with erythrocyte lysis buffer (154

mM NH_4Cl, 10 mM $KHCO_3$, 0.1 mM EDTA) and filtration using 40 μm cell strainers (BD Biosciences). Cells were resuspended in washing buffer consisting of PBS with 0.5% BSA and stained with antibodies for 1 h at 4°C. Cell sorting was performed on a FACSAria III 4L (BD Biosciences). Myogenic progenitors were isolated from live cell population (7-AAD$^-$) based on positive staining for α7-integrin and absence of Sca1, CD31 and CD45 staining, while fibro/adipogenic progenitors were sorted based on positive staining for Sca1 and absence of staining for α7-integrin, CD31 and CD45. Isolation of myogenic progenitors from human samples was based on CD56 expression and absence of CD15, CD31 and CD45 staining. Antibodies and respective dilutions used for cell stainings are listed in *SI Appendix*, Table S3. For isolation of stromal vascular fraction (SVF), adipose tissue from subcutaneous (inguinal), visceral (epididymal), or brown (interscapular) fat pads was dissected, minced, and digested in collagenase buffer for 1 h at 37°C in a shaking water bath. Cells were washed with DMEM supplemented with 10% FBS, filtered through a 40 μm cell strainer, and treated with erythrocyte lysis buffer before plating.

Cell culture. HEK 293/T17 and C2C12 cells were cultured in DMEM supplemented with 10% FBS (Gibco) and 1% penicillin/streptomycin (P/S, Gibco). Primary human and mouse myoblasts were cultured on collagen-coated plates in 1:1 v/v DMEM and Ham´s F-10 Nutrient Mix (Gibco) containing 20% FBS, 1% P/S and 5 ng/mL recombinant human FGF-2 (Gibco). Differentiation was initiated when myoblasts reached subconfluency by changing the media to DMEM containing 2% horse serum (Gibco) and 1% P/S. Experiments with myotubes were initiated after 4 days under low-serum conditions, when myoblasts were fully differentiated. SVF and 3T3-L1 cells were cultured on collagen-coated plates in DMEM supplemented with 10% FBS and 1% P/S. FAPs were grown on collagen-coated plates in DMEM containing 20% FBS, 1% P/S and 5 ng/mL recombinant human FGF-2. All cell cultures were incubated in a 37 °C 5% CO_2 water-jacketed incubator. For miR-29a overexpression, cells were transfected with 30 nM MISSION microRNA Mimic (Sigma) or MISSION miRNA Negative Control (Sigma). For miR-29a inhibition, cells were transfected with 12 nM antagomirs or respective control antagomirs. Antagomirs were designed as previously described (3) and custom synthesized by Sigma. For RNAi, 2 μg/mL of esiRNA (Sigma) targeting mouse Fosl1, mouse Sparc, human SPARC or a control esiRNA targeting GFP were transfected into muscle cells and, when indicated, treated with 0.58 nM FGF-2 or BSA for 48 h. Transfections of all oligonucleotides were performed using Lipofectamine RNAiMAX (Invitrogen) according to the manufacturer`s protocol. For Fosl1 overexpression, 2 μg/mL of pCDNA3-Fosl1 or pCDNA3 vectors were transfected using Lipofectamine 2000 (Invitrogen). Cells were lysed 48 h post-

transfection for RNA analysis and 72 h post-transfection for protein extraction. For recombinant protein treatments, 0.58 nM FGF-2, 50 µM dexamethasone (Sigma), 2.7 nM Wnt-3a, 0.58 nM TNF-a, 20 nM GDF-8, or 100 nM IGF-1 (all purchased from PeproTech) dissolved in starvation medium containing 0.5% FBS was used. Starvation medium supplemented with respective recombinant proteins was changed after 24 h. For inhibition of MEK1/2 signaling, cells were treated with 10 µM PD184352 (Selleckchem) in the presence of 0.58 nM FGF-2. Unless otherwise indicated, cells were lysed for RNA analysis after 48 h. For p-FRA-1 time course, human primary muscle cells were starved o/n with 1:1 v/v DMEM and Ham´s F-10 Nutrient Mix containing 1% P/S and subsequently treated with 0.58 nM FGF-2 dissolved in starvation medium. For viral Fosl1 or Fgf2 overexpression, mouse primary myoblasts were transduced in differentiation medium with adeno-associated viruses (AAVs) expressing Fosl1, Fgf2 or GFP at 7.5×10^{10} vg/well of a 24-well plate. Seven days post-infection, differentiated myotubes were analyzed for gene expression. For recombinant SPARC treatment, FAPs were seeded at a density of 1.6×10^5 cells per 12-well. 72h after FAPs reached confluency, adipogenic differentiation was induced using DMEM with 10% FBS and 1% P/S, supplemented with 500 mM IBMX, 1 µM dexamethasone and 172 nM insulin (all purchased from Sigma). Two days after induction, cells were cultured in insulin medium (DMEM containing 10% FBS, 1% P/S, 172 nM insulin) for 48 h; subsequently, cells were kept in DMEM supplemented with 10% FBS and 1% P/S. Respective media were supplemented with 1 µg/mL (4) recombinant SPARC (PeproTech) and refreshed each day. For co-cultures, muscle cells were seeded at a density of 1.5×10^5 (C2C12), 4×10^5 (mouse primary), or 1×10^5 (human primary) per 4.2 cm^2 cell growth area on transparent PET Membranes (Corning) with 1 µm pore size. Preadipocytes were seeded at a density of 4×10^5 cells (3T3-L1) or 3×10^5 cells (FAPs) per 6-well on Cell Culture Insert Companion plates (Corning). Transfections of muscle cells were performed 48 h prior to induction of adipogenic differentiation as described before. 72 h after preadipocytes reached confluency, adipogenic differentiation was induced as described before and mouse primary, human primary, C2C12, C2C12-Sparc$^{\Delta MRE}$ or C2C12-Sparc^{wt} cells, when indicated previously transfected with antagomirs or esiRNA, were cultured together with 3T3-L1 cells or FAPs for 8 days or 2 days in case of antagomir-29a transfected cells. All cells were harvested on day 8 after induction of adipogenesis for gene expression analysis or stained for differentiation analysis. For quantification of differentiation, cells were fixed with 4% formaldehyde for 20 min and washed 3 times with PBS. Immediately after washing, cells were stained with Bodipy 493/503 (Invitrogen) for lipid droplets and Hoechst dye (Cell Signaling) for nuclei. Twenty pictures per well were taken using the Cytation 5 Cell Imaging Multi Mode Reader (Biotek). Nuclei and lipid droplets were automatically analyzed using Gen5 software v3.08. For fibrogenic, smooth muscle,

and osteogenic differentiation, C2C12-Sparc$^{\Delta MRE}$ or C2C12-Sparc^{wt} and FAPs were plated as described before and co-cultured in DMEM, 5% horse serum, 1% P/S, supplemented with 5 ng/mL TGF-β1 (PeproTech) for 5 days or 0.5 µg/mL BMP-7 (PeproTech) for 4 days before gene expression analysis.

RNA extraction, cDNA synthesis, quantitative RT-PCR. Total RNA was isolated using TRIzol Reagent (Invitrogen) according to the manufacturer´s instruction. Traces of genomic DNA were removed using the DNA-free DNA Removal Kit (Invitrogen). Equal amounts of RNA were reverse-transcribed with random hexamer primers using SuperScript III First-Strand Synthesis System (Invitrogen). For miRNA qRT-PCR, 10 ng of total RNA was reverse-transcribed using the TaqMan MicroRNA Reverse Transcription Kit (Applied Biosystems). Quantitative RT-PCR for miRNA and mRNA levels were performed on a 7500 FAST Real-time PCR system (Applied Biosystems) using TaqMan Fast Universal PCR Master Mix, no AmpErase UNG (Applied Biosystems) and FastStart Universal SYBR Green Master (Roche), respectively. Gene expression was calculated using the Relative Standard Curve Method and 18S rRNA or Tbp, as indicated, for normalization. All primer sequences are given in *SI Appendix*, Table S2. The levels of miRNA were calculated using the ΔΔCt method and snoRNA234 or U6 snRNA for normalization. TaqMan assays for miR-29a (TM: 002112), snoRNA234 (TM: 001234), and U6 snRNA (TM: 001973) were purchased from Applied Biosystems.

Proliferation assay. Proliferation rates in genome-edited and wildtype C2C12 cells were measured using Click-iT EdU Alexa Fluor 488 Flow Cytometry Assay Kit (Invitrogen) according to manufacturer´s instruction. Briefly, transfected cells were treated with 5 µM EdU for 6 h. Cells were trypsinized and washed with 1% BSA in PBS. Cells were then fixed, permeabilized, and stained with the click reaction using Alexa Fluor 488 azide. Flow cytometry was performed on the LSR II Fortessa cell analyzer (BD Biosciences). Analysis and determining the percentage of EdU-positive cells was performed using FlowJo software (v10.6.2, BD Biosciences).

ELISA. SPARC levels in serum and cell culture supernatants were determined using the commercially available ELISA Kit for Osteonectin (Cloud-Clone Corp.). Colorimetric solutions were quantified using a PowerWave 340 Microplate Spectrophotometer (BioTek) and Gen5 software v1.11.

Plasmid construction. Wildtype Sparc 3´UTR was PCR-amplified from mouse cDNA using Phusion High-Fidelity DNA Polymerase (Invitrogen) and cloned into pCR2.1-TOPO using TOPO TA Cloning Kit (Invitrogen). Subsequently, Sparc 3´UTR was subcloned into pmirGLO Dual-Luciferase miRNA Target Expression Vector (Promega) downstream of the firefly luciferase ORF using T4 DNA Ligase (NEB). QuikChange II Site-Directed Mutagenesis Kit (Agilent Technologies) was used to generate miR-29a site mutations (M1, M2, M1M2) in pmirGLO-Sparc-3´UTR-wt. Human miR-29a promoter sequence was taken from Mott et al. (5). To generate pGL4.25-miR29a [-1493/+195], full-length promoter sequence was PCR-amplified from gDNA extracted from human myoblasts, with subsequent cloning into pCR2.1-TOPO and subcloning into pGL4.25 [*luc2CP*/minP] (Promega). Single promoter constructs were amplified from pGL4.25-miR29a [-1493/+195], cloned into pCR2.1-TOPO and ligated into pGL4.25 [*luc2CP*/minP]. Site-directed mutagenesis was used to generate the constructs M1, M2, and M3 from pGL4.25-miR29a [-374/-278]. To generate pCDNA3-Fosl1, the coding region of Fosl1 was PCR-amplified from mouse cDNA, cloned into PCR2.1-TOPO and ligated into pCDNA3. Site-directed mutagenesis was used to introduce the Kozak consensus sequence (5´-GCCGCCACCATGG-3´) in pCDNA3-Fosl1. To generate the AAV-Fosl1 plasmid, the ORF of Fosl1 was cloned from pCDNA3-Fosl1 into the KpnI/EcoRV sites of AAV-CAG-GFP replacing the eGFP element. To produce AAV-Fgf2, the Kozak consensus sequence was introduced into mFGF2 and the ORF of Fgf2 was subsequently cloned into the SpeI/EcoRV sites of AAV-Fosl1 replacing the Fosl1 element. To generate the AAV-Sparc plasmid, the coding region of Sparc was amplified from mouse cDNA and cloned into pCR2.1-TOPO. After introduction of the Kozak consensus sequence, the ORF was ligated into the BamHI/EcoRV sites of AAV-CAG-GFP replacing the eGFP element. All constructs were verified by Sanger Sequencing. All primers used for plasmid construction are listed in *SI Appendix*, Table S2. AAV-CAG-GFP (Addgene plasmid #28014) was a gift from Karel Svoboda (6). mFGF2 (Addgene plasmid #22084) was a gift from Gail Martin.

Luciferase assay. For Sparc 3´UTR reporter assay, C2C12 myoblasts were co-transfected with pmirGLO vector containing wildtype or mutated 3´UTRs and 30 nM MISSION miR-29a Mimics (Sigma) or MISSION miRNA Negative Control (Sigma). Transfected myoblasts were harvested 48 h post-transfection. For promoter bashing assays, respective wildtype or mutated miR-29a promoter constructs were co-transfected with pRL-TK (Promega), which provides constitutive expression of *Renilla* luciferase for internal control. After 24 h, medium was changed to differentiation medium. After 72 h, cells were treated with 0.58 nM FGF-2 or BSA until myotubes were collected at day 4 of differentiation. For Map2k2 overexpression assays, respective wildtype

or mutated miR-29a promoter constructs were triple-transfected with pRL-TK and pMCSG10-MKK2 or pCDNA3. Cells were differentiated and collected at day 4 of differentiation and when indicated treated with FGF-2, as described before. For Fosl1 overexpression assays, respective miR-29a promoter constructs were triple-transfected with pRL-TK and pCDNA3-Fosl1 or pCDNA3. C2C12 and mouse primary myotubes were treated with FGF-2 and collected, as described before. For inhibitor assays, respective promoter constructs were co-transfected with pRL-TK and treated with 0.1 µM PD173074, 10 µM PD184352, 50 µM NSC23766, 20 µM LY294002, 30 µM Nifuroxazide, 10 µM U73122 or DMSO when indicated together with 0.58 nM FGF-2 or BSA at day 3 of differentiation until myotubes were collected at day 4. All inhibitors were purchased from Selleckchem except for NSC23766 and Nifuroxazide (Sigma). For Fosl1 knockdown, pGL4.25-miR-29a [-374/-278] was triple-transfected with pRL-TK and 2 µg/mL esiRNA targeting Fosl1 or GFP. After 24 h, C2C12 culture medium was changed to differentiation medium supplemented with 0.58 nM FGF-2 or BSA and refreshed the next day. Myotubes were harvested 72 h post-transfection. All transfections were performed using Lipofectamine 2000 (Invitrogen). Luciferase reporter activity was measured using the Dual-Luciferase Reporter Assay System (Promega) on an Infinite 200 PRO multimode plate reader equipped with i-control software (Tecan). *Firefly* luciferase values were normalized to *Renilla* luciferase counts. pMCSG10-MKK2 (Addgene plasmid #29580) was a gift from Dustin Maly (7).

Genome editing. CRISPR-Cas9 was used to target DNA double-strand breaks (DSB) flanking the miR-29a recognition elements in the 3´UTR of Sparc and to stimulate genome editing via non-homologous end joining. crRNAs considering NGG protospacer adjacent motifs (PAMs) were designed using the miR-CRISPR tool (8). FastDigest BbiI (Thermo Scientific) and Quick Ligation Kit (NEB) were used to ligate the respective annealed oligonucleotide pairs into the BbsI sites of pSpCas9(BB)-2A-Puro (PX459) bearing both Cas9 and the remainder of the sgRNA as an invariant scaffold immediately following the cloning site. All constructs were verified by Sanger sequencing. C2C12 co-transfection with Lipofectamine 2000 (Invitrogen) was performed using the pSpCas9(BB)-2A-Puro plasmid expressing an sgRNA targeting the upstream sequence of MRE1 and a second pSpCas9(BB)-2A-Puro vector expressing one of two different sgRNAs targeting the downstream sequence of MRE2. Parallel application of two sgRNAs targeting the downstream sequence was chosen to facilitate a rapid screening of optimal candidate sgRNAs. Isolation of puromycin-resistant clonal cell lines was achieved by isolating single cells through serial dilutions followed by an expansion period. To screen cell lines for indel mutations, PCR was carried out on gDNA and visualized on a polyacrylamide TBE gel for the desired MRE disruption. Amplicons

were subcloned into pCR2.1-TOPO for transformation and individual colonies were Sanger sequenced to reveal the clonal genotype. Wildtype C2C12 cells serving as control lines were transfected with an empty pSpCas9(BB)-2A-Puro (PX459) vector and treated in the same way as the mutant cell lines. Primers and oligonucleotides used for genome editing are listed in *SI Appendix*, Table S2. pSpCas9(BB)-2A-Puro (PX459) (Addgene plasmid #48139) was a gift from Feng Zhang (9).

AAV9 production. To generate AAV-GFP, AAV-Fosl1, AAV-Sparc, and AAV-Fgf2, respective vectors were co-transfected together with pAdDeltaF6 helper and pAAV2/9n packaging plasmids in a 1:1:1 molar ratio using PEI transfection reagent (Polysciences). After 24 h, HEK 293T/17 cell culture medium was refreshed. Ninety-six hours post-transfection, cell culture medium was collected, centrifuged at 1,000 × g for 10 min, and filtered through a 0.45 µm PES membrane. Viral capsids were precipitated by adding 0.25 volumes of 40% polyethylene glycol 8000, pelleted at 1,500 × g for 30 min, resuspended in 200 µl PBS and stored at -80°C. For determination of AAV concentration, viral genomes were extracted with ViralXpress (Merck) and quantified by SYBR Green qPCR using priming sites for inverted terminal repeat (ITR) sequences. Primer sequences are provided in *SI Appendix*, Table S2. pAdDeltaF6 (Addgene plasmid #112867) and pAAV2/9n (Addgene plasmid #112865) were a gift from James M. Wilson.

Chromatin Immunoprecipitation. ChIP assays were performed on human primary myoblasts that were starved overnight and treated with 0.58 nM FGF-2 for 10 h while control cells received no FGF-2. ChIP assays on tissue samples were performed on excised gastrocnemius muscles from young or aged C57BL/6JRj mice. Assays were performed using the SimpleChIP Plus Enzymatic Chromatin IP Kit (Magnetic Beads) (Cell Signaling) according to the manufacturer´s instruction. Normal rabbit IgG antibody was included as negative control. DNA sequences were analyzed on a QuantStudio 5 Real-Time PCR System (Applied Biosystems) using FastStart Universal SYBR Green Master mix (Roche). The level of miR-29a promoter enrichment was determined relative to the total amount of input DNA (percent input method). For representative images, DNA sequences were amplified with standard PCR using GoTaq G2 Green master Mix (Promega) and visualized on an agarose gel. Full unedited gels are provided in *SI Appendix*, Fig S8 *C* and *D*. Primer sequences are provided in *SI Appendix*, Table S2. Antibodies are listed in *SI Appendix*, Table S3.

Protein extraction and western blot. Cells and skeletal muscle samples were lysed in RIPA Buffer (25 mM Tris HCl pH7.6, 150 mM NaCl, 1% NP-40, 1% sodium deoxycholate, 0.1% SDS)

supplemented with protease (Complete, Roche) and phosphatase (PhosSTOP, Roche) inhibitor cocktails. Lysates were cleared by centrifugation at 14,000 × g for 20 min at 4 °C. Protein concentrations were determined using Pierce BCA Protein Assay Kit (Thermo Sientific). Equal amounts of protein (25 µg) were separated by SDS-PAGE, transferred onto Protran Nitrocellulose Membranes (GE Healthcare) using eBlot L1 Fast Wet Transfer System (GenScript), followed by incubation with indicated primary antibodies according to manufacturer´s instruction. Signals of anti-rabbit IgG horseradish peroxidase-conjugated secondary antibodies were visualized on a LAS-3000 Luminescent Image Analyzer (Fujifilm) using Lumi-Light Western Blotting Substrate (Roche). Specific protein bands were densitometrically quantified using ImageJ (v 1.52q). Full unedited blots are provided in *SI Appendix*, Fig S8 *A*, *B* and *E*. All antibodies with respective dilutions are listed in *SI Appendix*, Table S3.

Histology. Mouse Tibialis anterior muscles and human biopsies from Tensor fasciae latae muscles were fixed in 4% formalin, and embedded in paraffin using the Excelsior AS Tissue Processor (Thermo Scientific). Sections of 4 µm thickness were prepared using a fully automated rotary microtome (RM2255, Leica Biosystems). Muscle tissue sections were deparaffinized, subjected to hematoxylin and eosin (H&E) staining and mounted in Pertex (Histolab). Human tissue sections were scanned using the Axio Scan.Z1 slidescanner (Zeiss) equipped with ZEN Imaging software v3.1. For each donor, 4 representative transverse sections obtained from two different parts of the biopsy were statistically analyzed. Murine tissue sections were scanned using the Cytation 5 Cell Imaging Multi Mode Reader (Biotek) equipped with Gen5 software v3.08. For AAV-Sparc infected aged mice, the Axio Scan.Z1 slidescanner was used. For each mouse, 3 representative transverse sections from the mid-belly of the muscles, each separated by 500 µm, were subjected to image and statistical analysis. For AAV-Sparc infected aged mice, 8 representative transverse sections separated by 250 µm were used. Intramuscular adipocytes were manually counted using the Cell Counting tool on ImageJ (v1.52q). Determination of total IMAT per section was performed by selecting the adipocytes using the Wand (tracing) tool and subsequent quantification of the area. For cross sectional area measurements of fibers, sections were de-paraffinized and rehydrated, stained with 5 µg/mL wheat germ agglutinin (WGA, Alexa Fluor 594 Conjugate, Invitrogen) and DAPI (1:1000, Invitrogen) for 15 min. For FAPs quantification, rehydrated sections were subjected to antigen retrieval using 10 mM tri-sodium citrate dihydrate, blocked (10% FBS, 1% Triton-X 100 in PBS) and incubated with anti-Pdgfrα primary antibody o/n at 4°C. Alexa Fluor 568-conjugated secondary antibody (Invitrogen) in combination with DAPI to visualize nuclei were subsequently applied for 1 h at room temperature. Sections were scanned using the Axio Scan.Z1 slidescanner

and for each mouse, four representative transverse sections from two different areas of the mid-belly of the muscles were analyzed. WGA or PDGFRα stained sections were thresholded and the Analyze Particle function in ImageJ was used to quantify fiber area and FAPs number, respectively. Colour coding of fiber area according to size was performed using the ROI Color Coder function (http://imagejdocu.tudor.lu/doku.php?id=macro:roi_color_coder). Representative images were captured using the Axio Imager 2 (Zeiss) equipped with an Axiocam 512 color camera (Zeiss) and ZEN Imaging software v3.1. All antibodies with respective dilutions are listed in *SI Appendix*, Table S3.

LC-MS/MS. For LC-MS/MS, serum free cell culture supernatants from C2C12 myotubes were collected 72 h post-transfection with antagomir-29a or control antagomirs. Label free quantification of secreted proteins was performed at the Functional Genomics Center Zurich. Briefly, proteins were precipitated using cold TCA/acetone, digested with trypsin and analyzed via LC-MS/MS using an Q Exactive Hybrid Quadrupole-Orbitrap Mass Spectrometer (Thermo Scientific). The acquired raw files were searched against MaxQuant database (09/02/16) using MaxQuant software v1.4.1.2. Variable modifications included oxidation (M), protein N-terminal acetylation, and deamidation (NQ). Protein FDR was set to 0.05. MaxQuant output was subjected to differential expression analysis using the Bioconductor package Limma.

RNA-seq. RNA-seq data were obtained from our previously published data set on human primary muscle cells derived from three healthy donors (10). Human myoblasts were transfected with antagomir-29a or control antagomir and 24h after transfection differentiation was induced for two days. After RNA isolation, RNA quality control was performed on the 4200 TapeStation system (Agilent). Sequencing libraries were prepared from 500 ng total RNA using the TruSeq Stranded mRNA Library Prep kit (Illumina) according to manufacturer´s instruction. Illumina flow cells were prepared and samples sequenced on an Illumina NovaSeq 6000 instrument to generate 100 bp single-end reads. RNA-seq reads were aligned with STAR-aligner using the gene annotation as provided by ENCODE release 91. Gene expression values were computed with the function featureCounts from the R package Rsubread.

Gene set enrichment analysis. GSEA was performed on $\log_2$ fold change ranked lists of all non-filtered datasets obtained from RNA-seq and LC-MS/MS converted to gene symbols using GSEA v3.0 (GSEAPreranked). miR-29a-3p targets obtained from TargetScan v7.2 were used as gene set database.

Bioinformatic miR-29a promoter analysis. Transcription factor binding sites in the miR-29a promoter were identified using the JASPAR database (http://jaspar.genereg.net) (11) that comprises non redundant TF binding profiles of various species as position frequency matrices. The 54 nt long miR-29a promoter sequence: 5'-AGAGGAAATTGGTCACTGCGTGTCATCTCGAGGGGTGGTGATTCAGGGAGCAGG-3' was searched to identify potential TF binding motifs in mouse. The score of the sequence motif matching the transcription factor position weight matrix is the sum of $\log_2$ likelihoods. The relative score is defined as the ratio of matching score over maximum possible score of $\log_2$ likelihoods and represent the ratio of score of the sequence motif matching the TF over a hypothetical sequence motif perfectly matching the TF binding profile (12).

Statistical analysis. Numerical values are reported as mean ± SEM. Sample sizes were determined on the basis of previous experiments and publications using similar methodologies as well as on observed effect sizes. For *in vivo* studies, littermates were randomly assigned to treatment groups whenever possible or were age-matched. Cell culture experiments were independently reproduced 2-3 times using different passage numbers. Statistical significance ($*p \leq 0.05$; $**p \leq 0.01$; $***p \leq 0.001$) was evaluated as specified in the figure legends using GraphPad Prism v8.4.2.

Study Approval. The human study was approved by the ethics committee of the Canton of Zurich (BASEC Nr 2017-01517) and all patients provided written informed consent prior to inclusion in the study. All animal procedures were approved by the Veterinary office of the Canton of Zurich.

Supplementary figures

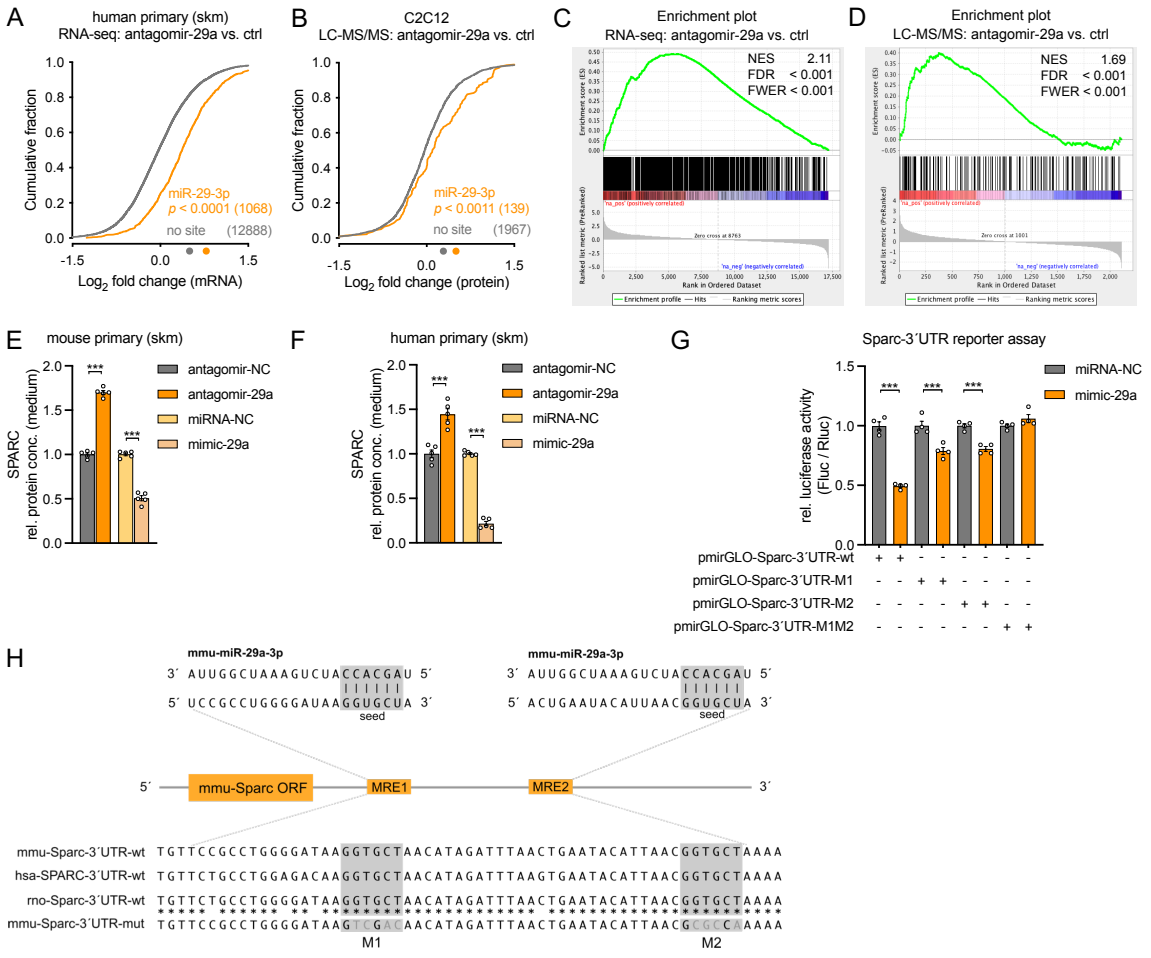

Fig. S1. Sparc is a conserved target of miR-29a. (***A***, ***B***) Cumulative distributions of ***A*** RNA-seq $\log_2$ FC in human myotubes (n = 3) or ***B*** LC-MS/MS $\log_2$ FC in C2C12 myotubes (n = 4). Similarity of miR-29a site-containing distributions (orange) to no-site distribution (grey) was tested. (***C***, ***D***) GSEA (Gene Set Enrichment Analysis) of predicted miR-29a targets (black lines) in $\log_2$FC ranked lists of non-filtered ***C*** RNA-seq (n = 3) or ***D*** LC-MS/MS (n = 4) datasets. NES = normalized enrichment score, FDR = false discovery rate; FWER = familywise-error rate. (***E***, ***F***) Levels of secreted SPARC in conditioned medium from ***E*** mouse primary myotubes, and ***F*** human primary myotubes after inhibition or overexpression of miR-29a as assessed by ELISA (n = 5). SPARC levels are plotted relative to negative control-antagomir or -mimic. (***G***) Normalized luciferase assay for wt Sparc 3´UTR and Sparc 3´UTR harboring mutations either in miR-29a recognition element (MRE) 1 (M1), MRE2 (M2) or both (M1M2), performed in C2C12 myotubes with overexpression of miR-29a (n = 4). (***H***) Nucleotide pairing of miR-29a seed regions to MRE1 and MRE2 located in the 3´UTR of Sparc (shaded boxes) is conserved between mouse, human, and rat. Stars indicate identical nucleotides among species. Nucleotides in grey represent mutated bases that were introduced to abolish miR-29a seed-pairing to mutant 1 (M1) and / or mutant 2 (M2) used in ***G***. Data in ***E-G*** are plotted as mean ± SEM. Significance was evaluated by ***A***, ***B*** one-sided Kolmogorov-Smirnov (K-S) test, ***E***, ***F*** two-tailed unpaired Student´s t test, ***G*** one-way ANOVA with Tukey´s multiple comparisons test. ***$p \leq 0.001$.

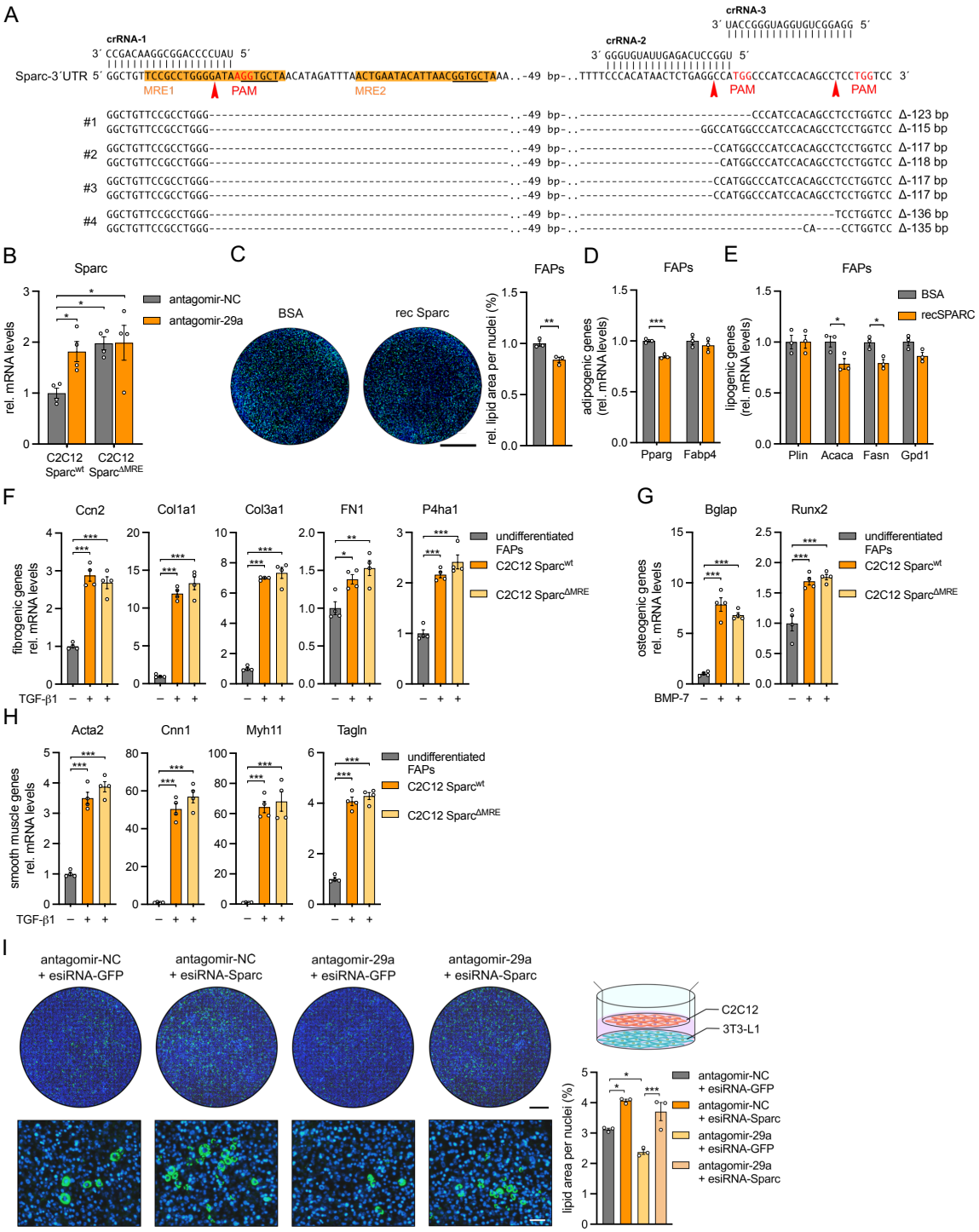
A
crRNA-1
crRNA-2
crRNA-3
Sparc-3´UTR
MRE1
MRE2
PAM
#1
#2
#3
#4
Δ-123 bp
Δ-115 bp
Δ-117 bp
Δ-118 bp
Δ-117 bp
Δ-117 bp
Δ-136 bp
Δ-135 bp
B
Sparc
rel. mRNA levels
antagomir-NC
antagomir-29a
C2C12 Sparcwt
C2C12 SparcΔMRE
C
BSA
rec Sparc
FAPs
rel. lipid area per nuclei (%)
D
FAPs
adipogenic genes (rel. mRNA levels)
Pparg
Fabp4
E
FAPs
BSA
recSPARC
lipogenic genes (rel. mRNA levels)
Plin
Acaca
Fasn
Gpd1
F
Ccn2
Col1a1
Col3a1
FN1
P4ha1
fibrogenic genes rel. mRNA levels
TGF-β1
undifferentiated FAPs
C2C12 Sparcwt
C2C12 SparcΔMRE
G
Bglap
Runx2
osteogenic genes rel. mRNA levels
BMP-7
H
Acta2
Cnn1
Myh11
Tagln
smooth muscle genes rel. mRNA levels
I
antagomir-NC + esiRNA-GFP
antagomir-NC + esiRNA-Sparc
antagomir-29a + esiRNA-GFP
antagomir-29a + esiRNA-Sparc
C2C12
3T3-L1
lipid area per nuclei (%)

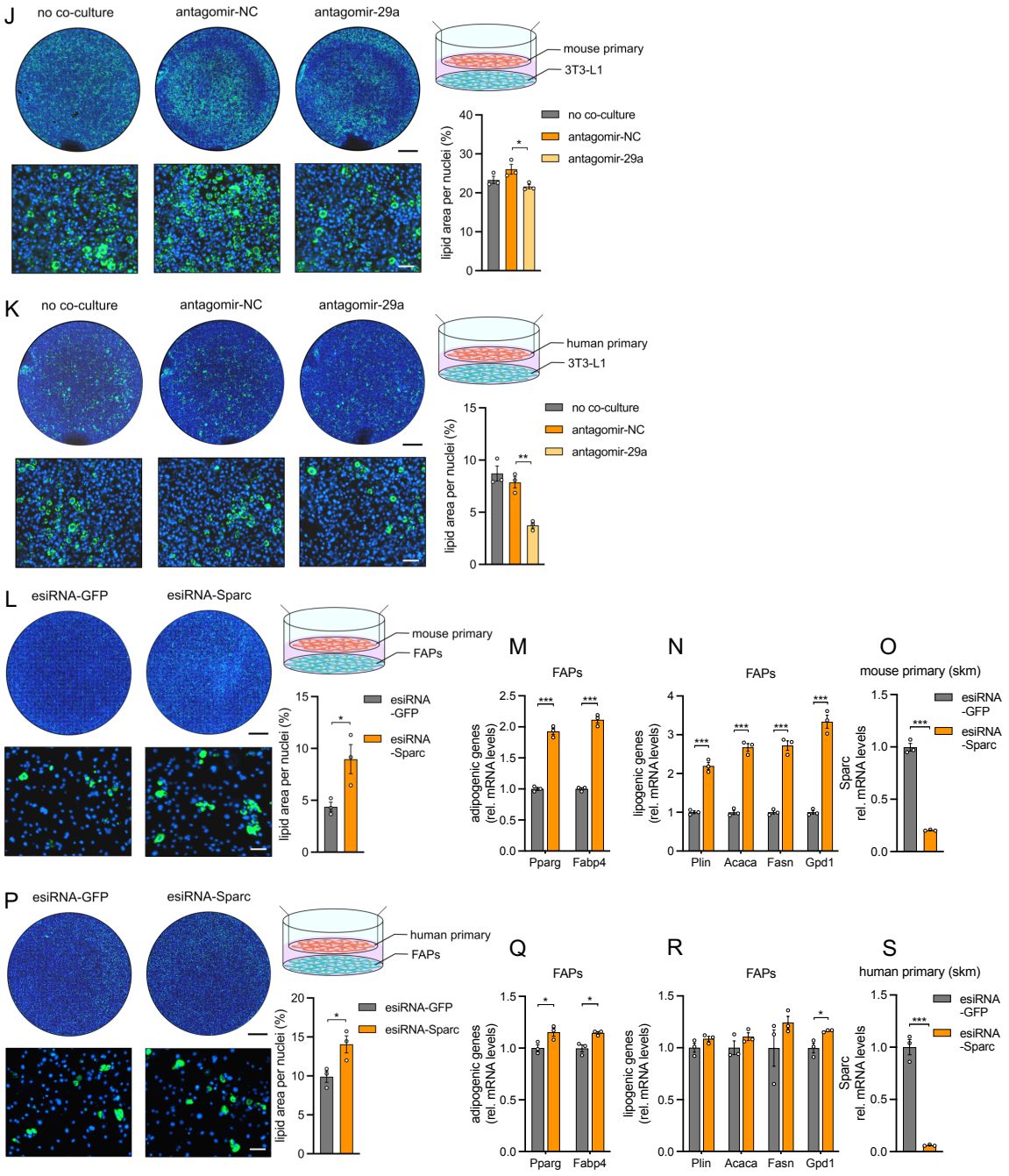

Fig. S2. The miR-29a/SPARC axis regulates adipogenesis but does not affect fibrogenic, osteogenic, or smooth muscle differentiation of FAPs. (***A***) Generation of deletions of miR-29a recognition elements (MRE) in C2C12 genomic Sparc 3´UTR using CRISPR/Cas9 editing (C2C12 Sparc$^{\Delta MRE}$ #1-4). Cas9 nuclease was targeted to Sparc 3´UTR by 20-nt guide sequences (crRNA) pairing directly upstream of a requisite 5´-NGG adjacent motif (PAM; red). Cas9 mediated a DSB ~3 bp upstream of the PAM (red arrowheads). Targeted miR-29a seed regions are underlined. (***B***) Sparc expression in wt or C2C12 myotubes with deleted miR-29a recognition elements (C2C12 Sparc$^{\Delta MRE}$) after inhibition of miR-29a (n = 4). (***C-E***) Treatment of Faps with 1 µg/mL recombinant Sparc for 8 days during adipogenesis (n = 3). ***C*** Representative images show lipid droplet (Bodipy; green) and nuclei (Hoechst; blue) staining of FAPs on day 8 after induction of adipogenesis.

Relative lipid area was normalized to nuclei. Scale bar, 5 mm. ***D***, ***E*** Adipogenic and lipogenic gene expression of FAPs treated with 1 µg/mL recombinant Sparc for 8 days during adipogenesis. (***F***-***H***) Expression of ***F*** fibrogenic genes, ***G*** osteogenic genes, and ***H*** smooth muscle genes in FAPs, co-cultured with C2C12 $Sparc^{wt}$ or C2C12 $Sparc^{\Delta MRE}$ cells and treated with 5 ng/mL TGF-β1 or 0.5 µg/mL BMP-7 (n = 4). RNA extracted from undifferentiated FAPs w/o C2C12 co-culture was used as control. (***I***-***K***) Co-culture of ***I*** C2C12, ***J*** mouse primary, or ***K*** human primary myotubes transfected as indicated with antagomir negative control (NC), antagomir-29a, esiRNA-GFP, and esiRNA-Sparc, and 3T3-L1 cells (n = 3). No co-culture control in ***J***, ***K*** shows 3T3-L1 cells cultured w/o primary myotubes. Representative images show lipid droplet (Bodipy; green) and nuclei (Hoechst; blue) staining of 3T3-L1 cells on day 8 after induction of adipogenesis. Lipid area was normalized to nuclei. Scale bar, 5 mm (top); 100 µm (bottom). (***L***-***S***) Co-culture of ***L***-***O*** mouse primary or ***P***-***S*** human primary myotubes transfected with esiRNA-GFP or esiRNA-Sparc, and FAPs (n = 3). Representative images show lipid droplet (Bodipy; green) and nuclei (Hoechst; blue) staining of FAPs on day 8 after induction of adipogenesis. Lipid area was normalized to nuclei. Scale bar, 5 mm (top); 100 µm (bottom). ***M***, ***Q*** adipogenic and ***N***, ***R*** lipogenic gene expression in FAPs co-cultured with esiRNA-GFP or esiRNA-Sparc transfected primary myotubes on day 8 after induction of adipogenesis. ***O***, ***S*** Sparc expression in esiRNA-GFP or esiRNA-Sparc transfected primary myotubes co-cultured with FAPs on day 8 after induction of adipogenesis. All qPCR values were normalized to 18S rRNA. All data are plotted as mean ± SEM. Significance was evaluated by ***B***, ***F***-***K*** one-way ANOVA with Dunnett´s (***B***) or Tukey´s (***F***-***K***) multiple comparisons test, ***C***-***E***, ***L***-***S*** two-tailed unpaired Student´s t test. $*p \leq 0.05$; $**p \leq 0.01$; $***p \leq 0.001$.

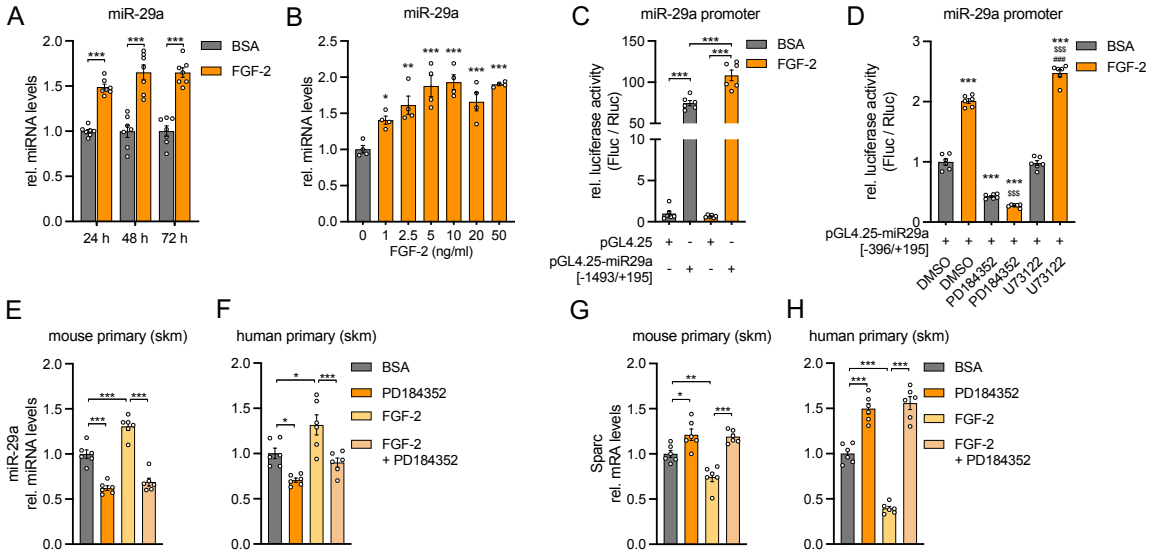

Fig. S3. Expression of miR-29a is mediated by FGF-2 and MEK1/2. (***A***) Time course of miR-29a expression after treatment with recombinant FGF-2 for indicated time points (n = 7). (***B***) Dose curve of miR-29a expression with indicated concentrations of recombinant FGF-2 treatment (n = 4). (***C***) miR-29a promoter activity for full-length (-1493/+195) promoter construct or empty vector after treatment with recombinant FGF-2 (n = 6). (***D***) miR-29a promoter activity for truncated (-396/+195) promoter construct after treatment with inhibitors against MEK1/2 (PD184352) or PLC (U73122) and recombinant FGF-2. * significantly different to DMSO + BSA, $ significantly different to DMSO + FGF-2, # significantly different to U73122 + BSA. Experiments in ***C***, ***D*** were performed in C2C12 myotubes and assessed by normalized luciferase assays (n = 6). (***E-H***) ***E***, ***F*** miR-29a and ***G***, ***H*** Sparc expression in ***E***, ***G*** mouse primary myoblasts, and ***F***, ***H*** human primary myoblasts after treatment with recombinant FGF-2 and inhibition of MEK1/2 signaling (PD184352; n = 6). qPCR values in ***A***, ***B***, ***E-H*** were normalized to snoRNA234 (miR-29a) or 18S rRNA (Sparc). All data are plotted as mean ± SEM. Significance was evaluated by ***A-H*** one-way ANOVA with Tukey´s (***A***, ***C-H***) or Dunnett´s (***B***) multiple comparisons test. *$p \leq 0.05$; **$p \leq 0.01$; ***$p \leq 0.001$.

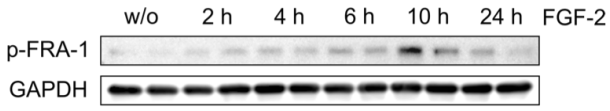

Fig. S4. FGF-2 increases the abundance of phosphorylated FRA-1. Representative immunoblot depicting phosphorylation of FRA-1 in human primary myoblasts treated with recombinant FGF-2 for indicated time points. GAPDH is shown as internal control (n = 2).

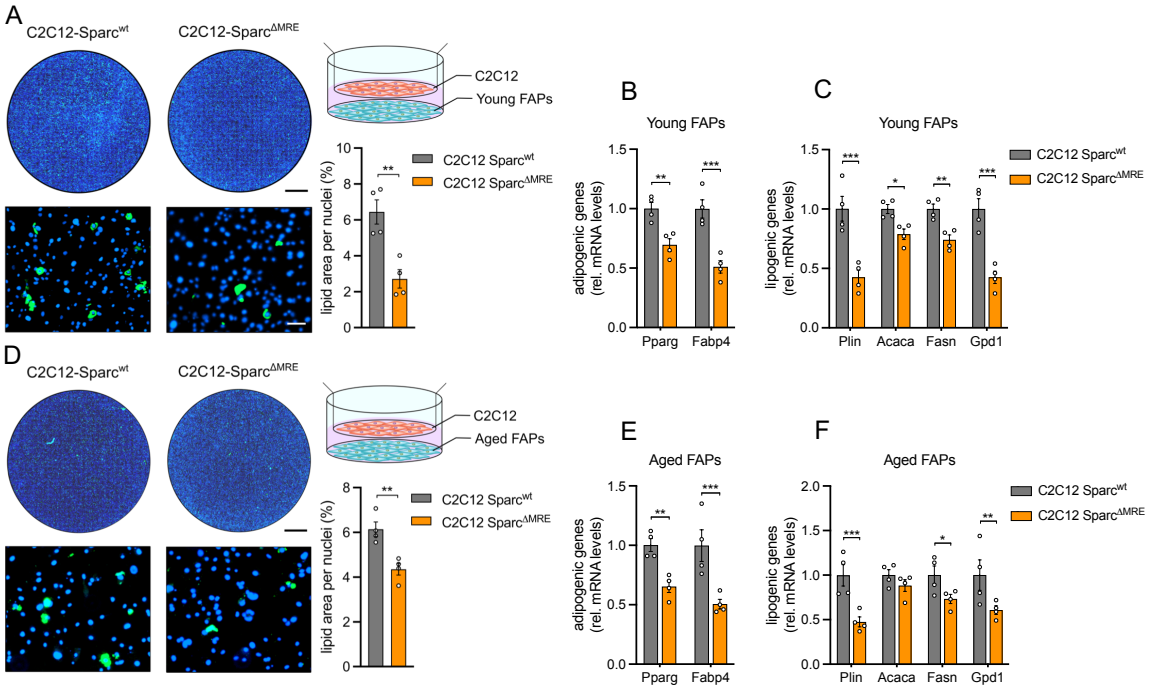

Fig. S5. FAPs isolated from aged mice retain sensitivity to SPARC induced inhibition of adipogenesis. (***A-F***) Co-culture of one clone of either wt or C2C12 myotubes with deleted miR-29a recognition elements (C2C12 Sparc$^{\Delta MRE}$) and fibro/adipogenic progenitor cells (FAPs) isolated from four 2 months (young) or four 25 months old (aged) mice (n = 4). ***A***, ***D*** Representative images show lipid droplet (Bodipy; green) and nuclei (Hoechst; blue) staining of FAPs on day 8 after induction of adipogenesis. Lipid area was normalized to nuclei. Scale bar, 5 mm (top); 100 µm (bottom). ***B***, ***E*** adipogenic and ***C***, ***F*** lipogenic gene expression of FAPs co-cultured with C2C12 Sparc^{wt} or C2C12 Sparc$^{\Delta MRE}$ myotubes on day 8 after induction of adipogenesis. qPCR values were normalized to 18S rRNA. All data are plotted as mean ± SEM. Significance was evaluated by ***A-F*** two-tailed unpaired Student´s t test. *$p \leq 0.05$; **$p \leq 0.01$; ***$p \leq 0.001$.

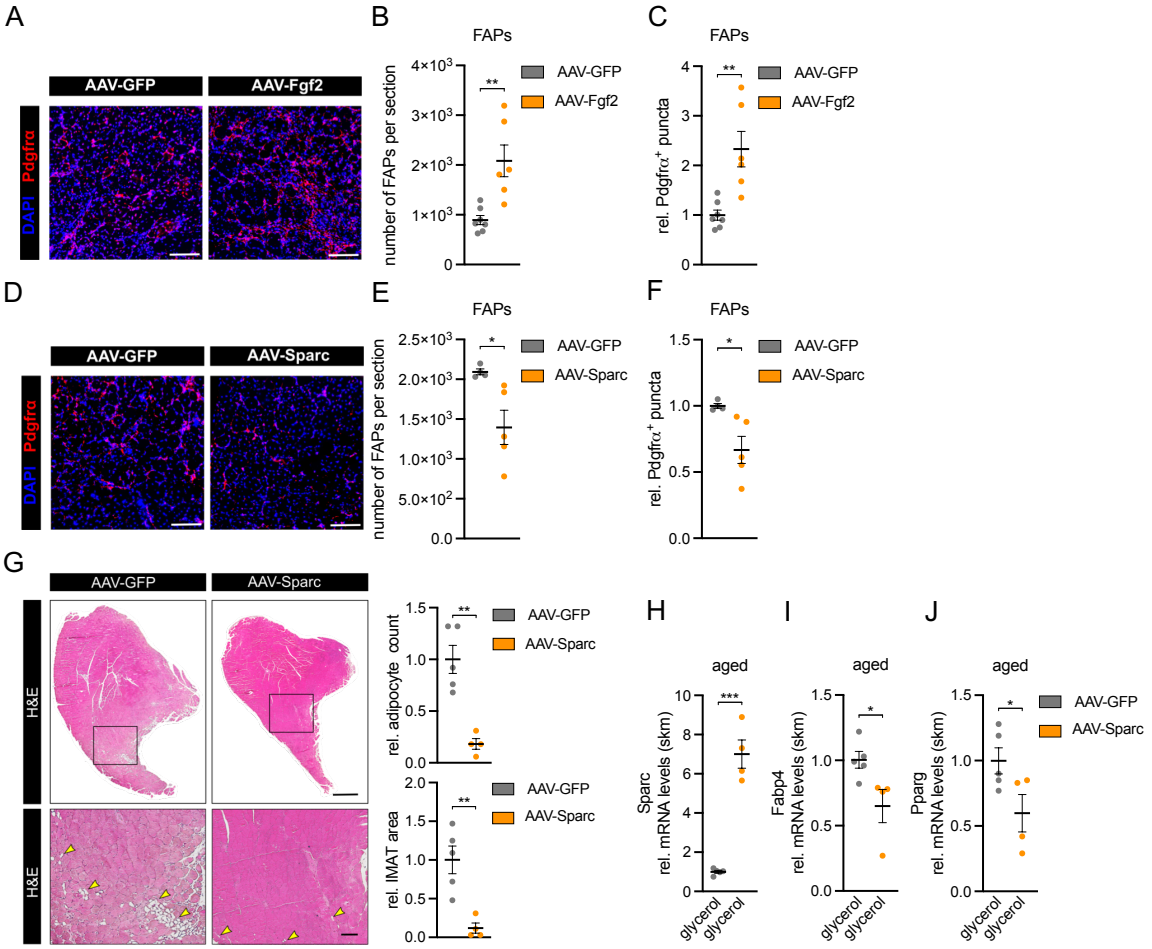

Fig. S6. The FGF-2/SPARC axis controls the number of FAPs and regulates aging-related IMAT. (***A***, ***D***) Representative immunofluorescence for FAPs (Pdgfra, red) in ***A*** AAV-Fgf2 (n = 7 vs. 6) or ***D*** AAV-Sparc (n = 4 vs. 5) infected tibialis anterior muscle two weeks after glycerol injection. Scale bar, 100 µm. (***B***, ***E***) Quantification of Pdgfra$^+$ cells present per section in ***B*** AAV-Fgf2 or ***E*** AAV-Sparc infected tibialis anterior muscle two weeks after glycerol injection. (***C***, ***F***) analysis of Pdgfra$^+$ puncta in ***C*** AAV-Fgf2 or ***F*** AAV-Sparc infected tibialis anterior muscle two weeks after glycerol injection. (***G***) Intramuscular adipose tissue (IMAT) formation in representative H&E staining of transverse sections in AAV-Sparc infected 25 months old tibialis anterior muscle two weeks after glycerol injection and analysis of relative IMAT area and adipocyte count (n = 5 vs. 4). Intramuscular adipocytes are indicated by yellow arrowheads. Scale bar, 0.5 mm (top); 100 µm (bottom) (***H-J***) ***H*** Sparc, ***I*** Fabp4, and ***J*** Pparg expression in AAV-Sparc infected tibialis anterior muscle two weeks after glycerol injection. qPCR values were normalized to Tbp. All data are plotted as mean ± SEM. Significance was evaluated by ***B***, ***C***, ***E-J*** two-tailed unpaired Student´s t test. *$p \leq 0.05$; **$p \leq 0.01$; ***$p \leq 0.001$.

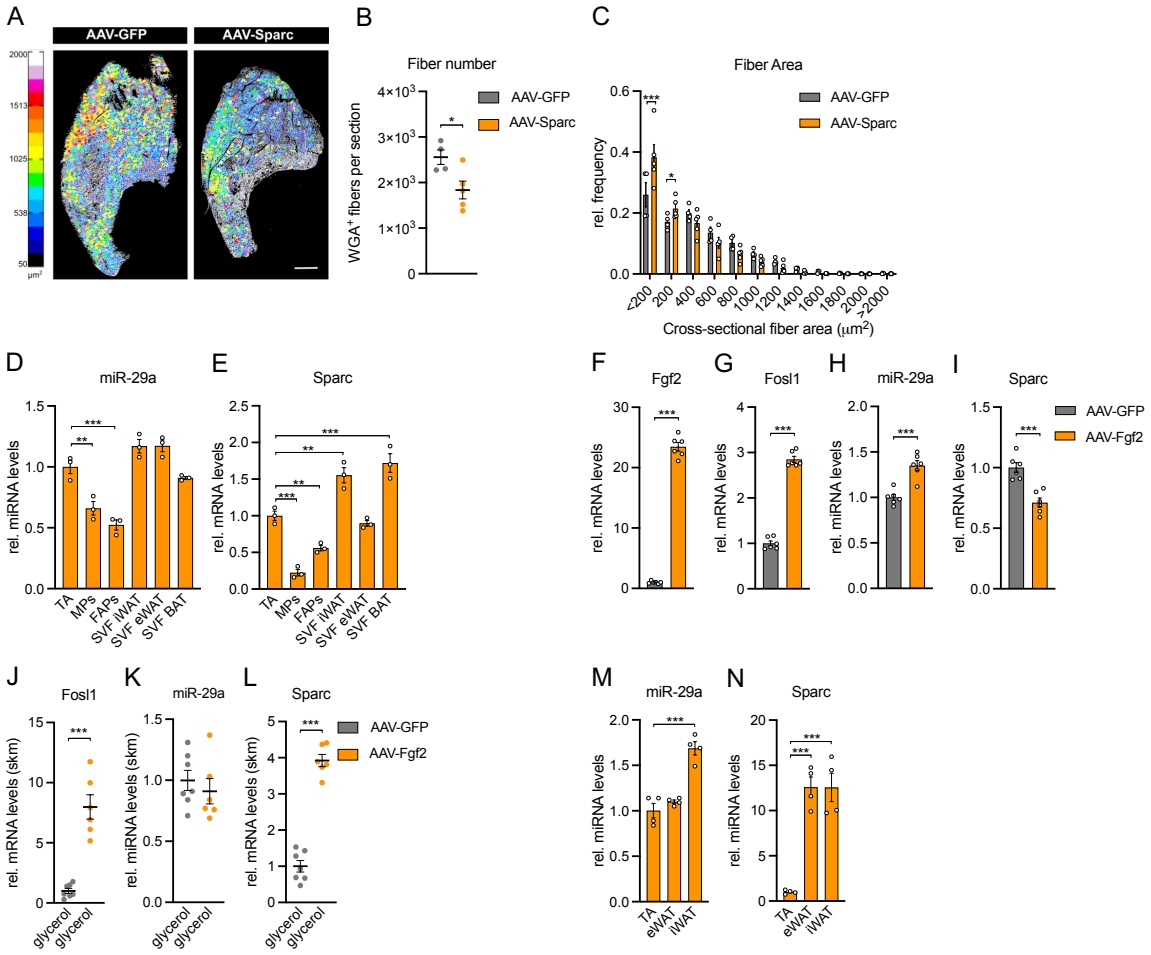

Fig. S7. Sparc decreases fiber number and is differentially expressed in progenitor cells, white adipose tissue and muscle. (***A***) Representative wheat germ agglutinin (WGA) staining of myofibers from AAV-Sparc infected tibialis anterior muscle two weeks after glycerol injection, color-coded based on size of cross-sectional area using the ROI Color Coder function in ImageJ. Scale bar, 0.5 mm. (***B***) Quantification of the number of myofibers present per section in AAV-Sparc infected tibialis anterior muscle two weeks after glycerol injection (n = 4 vs. 5). (***C***) Relative frequency distribution of fibers based on their cross-sectional area in AAV-Sparc infected tibialis anterior muscle two weeks after glycerol injection (n = 4 vs. 5). (***D***, ***E***) ***D*** miR-29a and ***E*** Sparc expression in tibialis anterior muscle compared to myogenic progenitors (MPs), fibro/adipogenic progenitors (FAPs), stromal vascular fraction (SVF) of inguinal white adipose tissue (iWAT), epididymal white adipose tissue (eWAT), and brown adipose tissue (BAT) isolated from male C57BL/6J mice and cultured for 48h before RNA extraction (n = 3). (***F-I***) ***F*** Fgf2, ***G*** Fosl1, ***H*** miR-29a, and ***I*** Sparc expression in mouse primary myotubes 7 days after AAV-mediated overexpression of Fgf2 (n = 6). (***J-K***) ***J*** Fosl1, ***K*** miR-29a, and ***L*** Sparc expression in AAV-Fgf2 infected tibialis anterior muscle two weeks after glycerol injection (n = 7 vs. 6). (***M***, ***N***) ***M*** miR-29a and ***N*** Sparc expression in tibialis anterior muscle, epididymal white adipose tissue (eWAT) and inguinal white adipose tissue (iWAT) from male C57BL/6J mice (n = 4). All qPCR values were normalized to 18S rRNA or snoRNA234 (miR-29a). All data are plotted as mean ± SEM. Significance was evaluated by ***B***, ***F-L*** two-tailed unpaired Student´s t test, ***C*** two-way ANOVA with Fisher´s LSD multiple comparisons test, ***D***, ***E***, ***M***, ***N*** one-way ANOVA with Dunnett´s multiple comparisons test. *$p \leq 0.05$; **$p \leq 0.01$; ***$p \leq 0.001$.

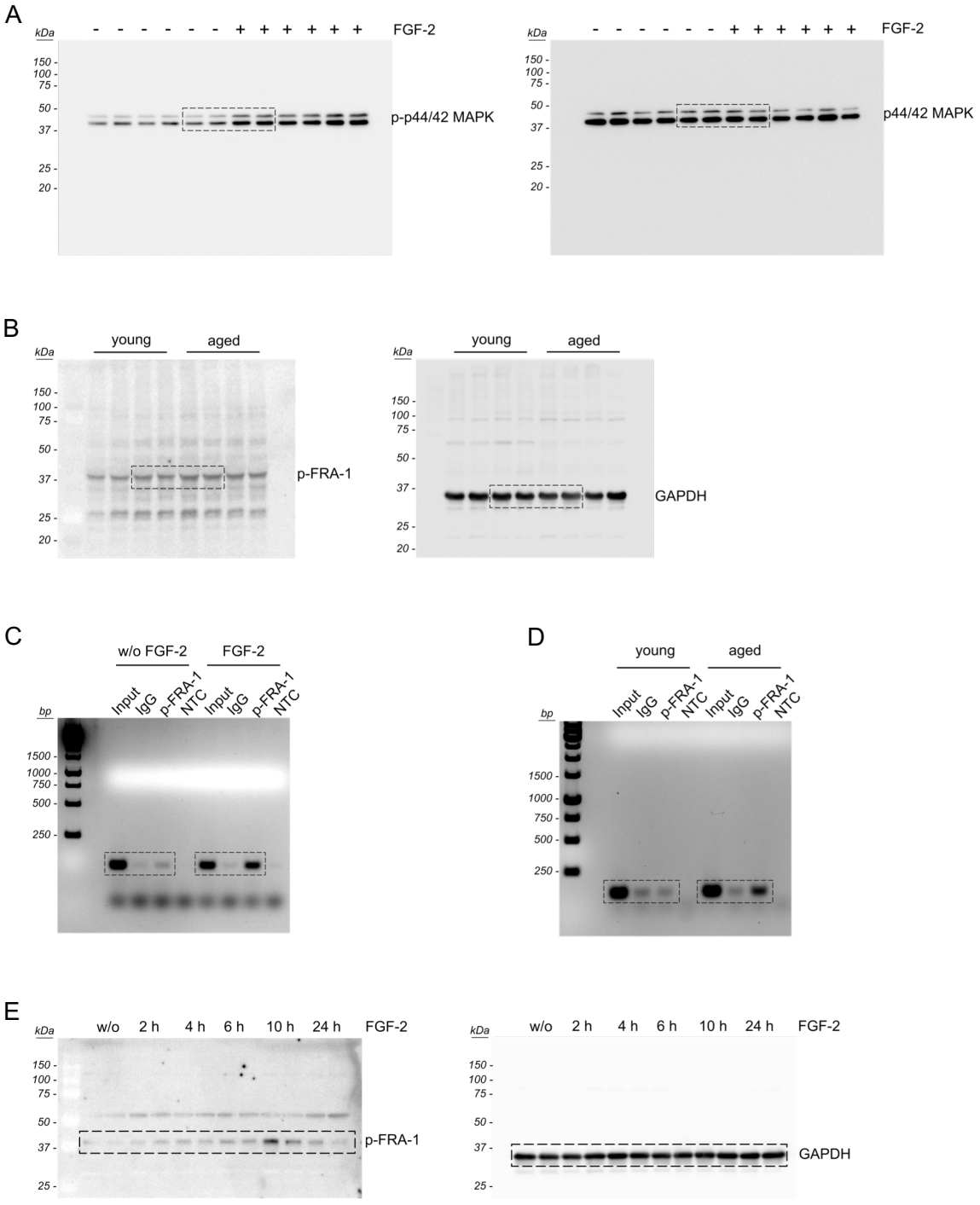

Fig. S8. Full unedited blots and gels. (***A***) Full unedited blot of Fig. 3G. (***B***) Full unedited blot of Fig. 5F. (***C***) Full unedited gel of Fig. 4P. (***D***) Full unedited gel of Fig. 5G. (***E***) Full unedited blot of Fig. S4.

Table S1. Secreted Proteins significantly changed after inhibition of miR-29a and their potential role in adipogenesis based on a literature search.

Gene	Protein	Log_2-FC	p-value	potential role in adipogenesis
Fstl1	Follistatin-related protein 1	1.146	0.0074	(13-16)
Cx3cl1	Fractalkine	1.048	0.0347	(17, 18)
Itgb1	Integrin beta-1	1.038	0.0324	(19)
Sparc	SPARC	1.037	0.0064	(4, 20-23)
Nasp	Nuclear autoantigenic sperm protein	0.962	0.0358	none
Rps6ka3	Ribosomal protein S6 kinase alpha-3	0.897	0.0158	(24)
Mmp2	72 kDa type IV collagenase	0.860	0.0181	(25-28)
F11r	Junctional adhesion molecule A	0.805	0.0303	none
Ccdc80	Coiled-coil domain-containing protein 80	0.695	0.0138	(29, 30)
Ehd2	EH domain-containing protein 2	0.605	0.0486	(31, 32)
Atp6v1a	V-type proton ATPase catalytic subunit A	-0.518	0.0341	none
Mat2a	S-adenosylmethionine synthase isoform type-2	-0.728	0.0379	(33, 34)
Sms	Spermine synthase	-0.922	0.0222	none

Data and color are related to Fig. 1*C*. The NCBI PubMed database was queried on April 26th 2021 using "*((Gene) OR (Protein)) AND ((adipogenic) OR (adipogenesis) OR (adipose tissue))"*

Table S2. List of oligonucleotides used in the present study.

Name	Sequence (5´→ 3´)	Application
m_ACTA1-Cre_1	FWD: CTAGGCCACAGAATTGAAAGATCT REV: GTAGGTGGAAATTCTAGCATCATCC	Genotyping
m_ACTA1-Cre_2	FWD: ATACCGGAGATCATGCAAGC REV: AGGTGGACCTGATCATGGAG	Genotyping
m_Pax7-cre_1	FWD: CTCCTCCACATTCCTTGCTC REV: CGGCCTTCTTCTAGGTTCTG	Genotyping
m_Pax7-cre_2	FWD: GCGGTCTGGCAGTAAAAACTATC REV: GTGAAACAGCATTGCTGTCACTT	Genotyping
m_miR29ab1	FWD: TGTGTTGCTTTGCCTTTGAG REV: CCACCAAGAACACTGATTTCAA	Genotyping
m_CRISPR-Cas9_1	FWD: CTGATGTGTCACCCCTCCCA REV: ATCTCCTCGTGCTTGTGGAC	Genotyping
m_CRISPR-Cas9_2	FWD: CTGGGGATAAGGTGCTAACA REV: ATCTCCTCGTGCTTGTGGAC	Genotyping
m_CRISPR-Cas9_3	FWD: ACATAACTCTGAGGCCATGGC REV: ACTTCCCTCTGCCTAACTCC	Genotyping
m_CRISPR-Cas9_4	FWD: CATCCACAGCCTCCTGGTCC REV: ACTTCCCTCTGCCTAACTCC	Genotyping
m_18S rRNA	FWD: GACACGGACAGGATTGACAGATTG REV: AAATCGCTCCACCAACTAAGAACG	qPCR
m_Sparc	FWD: TTCAGACCGCCAGAACTCTT REV: CCAGGCAAAGGAGAAAGAAG	qPCR
m_Fgf2	FWD: AGAAGAGCGACCCACACG REV: GGCACACACTCCCTTGATAGA	qPCR
m_Pparg	FWD: TGCTGTTATGGGTGAAACTCTG REV: CTGTGTCAACCATGGTAATTTCTT	qPCR
m_Fabp4	FWD: GATGAAATCACCGCAGACGACA REV: ATTGTGGTCGACTTTCCATCCC	qPCR
m_Tbp	FWD: CATCTCAGCAACCCACACAG REV: GGGGTCATAGGAGTCATTGG	qPCR
m_Fosb	FWD: TTTTCCCGGAGACTACGACTC REV: GTGATTGCGGTGACCGTTG	qPCR
m_Fos	FWD: CGGGTTTCAACGCCGACTA REV: TGGCACTAGAGACGGACAGAT	qPCR
m_Fosl1	FWD: ATGTACCGAGACTACGGGGAA REV: CTGCTGCTGTCGATGCTTG	qPCR
m_Fosl2	FWD: CACTCCCGGCACTTCAAAC REV: GAGTCTGATGACTGGTCCCC	qPCR
m_Jun	FWD: ACTCGGACCTTCTCACGTC REV: GGTCGGTGTAGTGGTGATGT	qPCR
m_JunD	FWD: GAAACGCCCTTCTATGGCGA REV: CAGCGCGTCTTTCTTCAGC	qPCR
m_Jdp2	FWD: AGCTGAAATACGCTGACATCC REV: CTCACTCTTCACGGGTTGGG	qPCR
m_Plin	FWD: CAAGCACCTCTGACAAGGTTC REV: GTTGGCGGCATATTCTGCTG	qPCR

m_Acaca	FWD: CGCCAACAATGGTATTGCAGC REV: TCGGATTGCACGTTCATTTCG	qPCR
m_Fasn	FWD: GTCGTCTGCCTCCAGAGC REV: GTTGGCCCAGAACTCCTGTA	qPCR
m_Gpd1	FWD: ATGGCTGGCAAGAAAGTCTG REV: CCTGCATTGCTACCCACGAT	qPCR
m_Ccn2	FWD: GGACACCTAAAATCGCCAAGC REV: ACTTAGCCCTGTATGTCTTCACA	qPCR
m_Col1a1	FWD: ACATGTTCAGCTTTGTGGACC REV: TAGGCCATTGTGTATGCAGC	qPCR
m_Col3a1	FWD: GGAACCTGGTTTCTTCTCACC REV: TAGGACTGACCAAGGTGGCT	qPCR
m_FN1	FWD: ACCTCTGCAGACCTACCCAG REV: TTGGTGATGTGTGAAGGCTC	qPCR
m_P4ha1	FWD: AGACCGGCTAACGAGTACAG REV: CCAACTCACTCCACTCAGTGT	qPCR
m_Bglap	FWD: GAACAGACAAGTCCCACACAGC REV: TCAGCAGAGTGAGCAGAAAGAT	qPCR
m_Runx2	FWD: AACGATCTGAGATTTGTGGGC REV: CCTGCGTGGGATTTCTTGGTT	qPCR
m_Acta2	FWD: GTCCCAGACATCAGGGAGTAA REV: TCGGATACTTCAGCGTCAGGA	qPCR
m_Cnn1	FWD: TCTGCACATTTTAACCGAGGTC REV: GCCAGCTTGTTCTTTACTTCAGC	qPCR
m_Myh11	FWD: CGGCAATGCGAAAACCGTC REV: AGTGACATCGAAGTTGATGCG	qPCR
m_Tagln	FWD: CAACAAGGGTCCATCCTACGG REV: ATCTGGGCGGCCTACATCA	qPCR
m_ChIP_promoter	FWD: TGGTCACTGCGTGTCATCTC REV: CTGCCCTCTGAGAAGTGAGC	qPCR
h_ChIP_promoter	FWD: CTGGTCATGGCGTGTCATCT REV: GCCTGCACTCTGAGAACTGA	qPCR
h_18SrRNA	FWD: GTAACCCGTTGAACCCCATT REV: CCATCCAATCGGTAGTAGCG	qPCR
h_SPARC	FWD: CTTCAGACTGCCCGGAGA REV: GAAAGAAGATCCAGGCCCTC	qPCR
h_FGF2	FWD: AGAAGAGCGACCCTCACATCA REV: CGGTTAGCACACACTCCTTTG	qPCR
h_PPARG	FWD: TACTGTCGGTTTCAGAAATGCC REV: GTCAGCGGACTCTGGATTCAG	qPCR
h_FOSL1	FWD: CAGGCGGAGACTGACAAACTG REV: TCCTTCCGGGATTTTGCAGAT	qPCR
h_FABP4	FWD: CCACCATAAAGAGAAAACGAGAG REV: GTGGAAGTGACGCCTTTCAT	qPCR
ITR	FWD: GGAACCCCTAGTGATGGAGTT REV: CGGCCTCAGTGAGCGA	qPCR
m_Sparc-3´UTR-wt	FWD: TCCTGAACTCTCTCCCTCTGA REV: AAGGTTTCAAGTGGCAGGGG	Cloning
h_miR29a-promoter [-1493/+195]	FWD: GAGTTGGGGTCTAAGTGGCA REV: ACCACCTACTCACCGAGTGT	Cloning

h_miR29a-promoter [-977/+195]	FWD: TTTCTACCCCTGTGATGGAC REV: ACCACCTACTCACCGAGTGT	Cloning
h_miR29a-promoter [-396/+195]	FWD: CCCATCGCAGAGGATTAGAC REV: ACCACCTACTCACCGAGTGT	Cloning
h_miR29a-promoter [-245/+195]	FWD: CAGAGGTTGCTGCTCACTTC REV: ACCACCTACTCACCGAGTGT	Cloning
h_miR29a-promoter [-396/-355]	FWD: CCCATCGCAGAGGATTAGAC REV: CCCTATGATCCATGCACCCT	Cloning
h_miR29a-promoter [-374/-312]	FWD: AGGGTGCATGGATCATAGGG REV: CGCAGTGACCAATTTCCTCT	Cloning
h_miR29a-promoter [-374/-278]	FWD: AGGGTGCATGGATCATAGGG REV: CCTGCTCCCTGAATCACCAC	Cloning
h_miR29a-promoter [-297/-226]	FWD: GTGGTGATTCAGGGAGCAGG REV: GAAGTGAGCAGCAACCTCTG	Cloning
m_Fosl1-ORF	FWD: TGTCTGTAGAGGCGGCTTGC REV: TTGCGGTGGAGGCTCGGATA	Cloning
m_Sparc-ORF	FWD: CTTCAGACCGCCAGAACTCTT REV: TAGCACCTTATCCCCAGGCG	Cloning
m_CRISPR-Cas9_5	FWD: GACACCCAGCCTCTGTTGTATTA REV: ACTTCCCTCTGCCTAACTCC	Cloning
m_Sparc-3´UTR-M1	FWD: GTTAATGTATTCAGTTAAATCTATGTTGTC GACTTATCCCCAGGCGGAACAGCCAACC REV: GGTTGGCTGTTCCGCCTGGGGATAAGTCG ACAACATAGATTTAACTGAATACATTAAC	site-directed mutagenesis
m_Sparc-3´UTR-M2	FWD: GAATACATTAACGGCGCCAAAAAAAAAA AAAAAACAAAGTAAGAAAGAAACTAGAACCCA AGTCAC REV: GTGACTTGGGTTCTAGTTTCTTTCTTACTT TGTTTTTTTTTTTTTTTTGGCGCCGTTAATGTATT C	Site-directed mutagenesis
h_miR29a-promoter [-374/-278]-M1	FWD: GGTTTTTGAACAGAAGGGAGTTTTAAGA GGAAATGAGCTCCTGCGTGTCATCTCGAGG REV: CCTCGAGATGACACGCAGGAGCTCATTTC CTCTTAAAACTCCCTTCTGTTCAAAAACC	Site-directed mutagenesis
h_miR29a-promoter [-1493/+195]-M2	FWD: CCCTGAATCACCACCCCTCGAGGAGCTC CGCAGTGACCAATTTCCTCTTA REV: TAAGAGGAAATTGGTCACTGCGGAGCTCC TCGAGGGGTGGTGATTCAGGG	Site-directed mutagenesis
h_miR29a-promoter [-1493/+195]-M3	FWD: CGCCCTTCCTGCTCCCTGAGAGCTCACCC CTCGAGATGACACG REV: CGTGTCATCTCGAGGGGTGAGCTCTCAGG GAGCAGGAAGGGCG	Site-directed mutagenesis
m_Fosl1-kozak	FWD: ACCCTACCGAACATCCAGCCGCCACCAT GGTCCGAGACTACGGGGAACCGG REV: CCGGTTCCCCGTAGTCTCGGACCATGGTG GCGGCTGGATGTTCGGTAGGGT	Site-directed mutagenesis
m_Sparc-kozak	FWD: CTGCCTGCCTGTGCCGAGAGTTGCCGCCA CCATGGTCGCCTGGATCTTCTTTCTCC REV: GGAGAAAGAAGATCCAGGCGACCATGGT GGCGGCAACTCTCGGCACAGGCAGGCAG	Site-directed mutagenesis

m-Fgf2-kozak	FWD: CCGCTGGCAGCCATGGTGGCGGCGCGGC GGGGGATCCA REV: TGGATCCCCCGCCGCGCCGCCACCATGGC TGCCAGCGG	Site-directed mutagenesis
m_crRNA-1	SENSE: CACCGGGCTGTTCCGCCTGGGGATA ANTISENSE: AAACTATCCCCAGGCGGAACAGC CC	CRISPR-Cas9
m_crRNA-2	SENSE: CACCGCCCACATAACTCTGAGGCCA ANTISENSE: AAACTGGCCTCAGAGTTATGTGGG C	CRISPR-Cas9
m_crRNA-3	SENSE: CACCGATGGCCCATCCACAGCCTCC ANTISENSE: AAACGGAGGCTGTGGATGGGCCAT C	CRISPR-Cas9

Table S3. List of antibodies used in the present study.

Name	Source	Supplier/Product#	Application
Alexa Fluor 488 anti-mouse CD45	Rat	BioLegend #103121	FACS (1:1,000)
Alexa Fluor 488 anti-mouse CD31	Rat	BioLegend #102414	FACS (1:1,000)
APC anti-mouse Ly-6A/E (Sca-1)	Rat	BioLegend #108111	FACS (1:1,000)
Alexa Fluor 488 anti-human CD45	Mouse	BioLegend #304019	FACS (1:100)
PE anti-human CD56 (NCAM)	Mouse	BioLegend #318305	FACS (1:100)
APC anti-human CD15 (SSEA-1)	Mouse	BioLegend #323007	FACS (1:2,000)
FITC anti-human CD31	Mouse	BioLegend #303103	FACS (1:5,000)
Anti-mouse Integrin alpha 7 PE-conjugated	Rat	R&D Systems #FAB3518P	FACS (1:100)
Normal Rabbit IgG	Rabbit	Cell Signaling #2729	ChIP (1:333)
Phospho-FRA1 (Ser265)	Rabbit	Cell Signaling #5841	ChIP (1:50) WB (1:1,000)
p44/42 MAPK	Rabbit	Cell Signaling #4695	WB (1:1,000)
Phospho-p44/42 MAPK (Thr202/Tyr204)	Rabbit	Cell Signaling #4370	WB (1:1,000)
GAPDH	Rabbit	Proteintech #10494-1-AP	WB (1:2,000)
Anti-Rabbit IgG Peroxidase Conjugate	Goat	Calbiochem #401393	WB (1:10,000)
Anti-Mouse PDGFRα	Goat	R&D Systems #AF1062	IF (1:200)
Anti-Goat IgG-Alexa Fluor 568	Donkey	Invitrogen #A-11057	IF (1:500)

SI References

1. K. M. Smith *et al.*, miR-29ab1 deficiency identifies a negative feedback loop controlling Th1 bias that is dysregulated in multiple sclerosis. *J Immunol* **189**, 1567-1576 (2012).
2. A. Galimov *et al.*, MicroRNA-29a in Adult Muscle Stem Cells Controls Skeletal Muscle Regeneration During Injury and Exercise Downstream of Fibroblast Growth Factor-2. *Stem Cells* **34**, 768-780 (2016).
3. J. Krutzfeldt *et al.*, Silencing of microRNAs in vivo with 'antagomirs'. *Nature* **438**, 685-689 (2005).
4. J. Nie, E. H. Sage, SPARC inhibits adipogenesis by its enhancement of beta-catenin signaling. *J Biol Chem* **284**, 1279-1290 (2009).
5. J. L. Mott *et al.*, Transcriptional suppression of mir-29b-1/mir-29a promoter by c-Myc, hedgehog, and NF-kappaB. *J Cell Biochem* **110**, 1155-1164 (2010).
6. T. Mao *et al.*, Long-range neuronal circuits underlying the interaction between sensory and motor cortex. *Neuron* **72**, 111-123 (2011).
7. S. B. Hari, E. A. Merritt, D. J. Maly, Sequence determinants of a specific inactive protein kinase conformation. *Chem Biol* **20**, 806-815 (2013).
8. A. R. Bassett *et al.*, Understanding functional miRNA-target interactions in vivo by site-specific genome engineering. *Nat Commun* **5**, 4640 (2014).
9. F. A. Ran *et al.*, Genome engineering using the CRISPR-Cas9 system. *Nat Protoc* **8**, 2281-2308 (2013).
10. E. Luca *et al.*, Genetic deletion of microRNA biogenesis in muscle cells reveals a hierarchical non-clustered network that controls focal adhesion signaling during muscle regeneration. *Mol Metab* **36**, 100967 (2020).
11. O. Fornes *et al.*, JASPAR 2020: update of the open-access database of transcription factor binding profiles. *Nucleic Acids Res* **48**, D87-D92 (2020).
12. W. W. Wasserman, A. Sandelin, Applied bioinformatics for the identification of regulatory elements. *Nat Rev Genet* **5**, 276-287 (2004).
13. D. Fang, X. Shi, T. Lu, H. Ruan, Y. Gao, The glycoprotein follistatin-like 1 promotes brown adipose thermogenesis. *Metabolism* **98**, 16-26 (2019).
14. V. Prieto-Echagüe *et al.*, BBS4 regulates the expression and secretion of FSTL1, a protein that participates in ciliogenesis and the differentiation of 3T3-L1. *Sci Rep* **7**, 9765 (2017).
15. N. Fan *et al.*, Follistatin-like 1: a potential mediator of inflammation in obesity. *Mediators Inflamm* **2013**, 752519 (2013).
16. Y. Wu, S. Zhou, C. M. Smas, Downregulated expression of the secreted glycoprotein follistatin-like 1 (Fstl1) is a robust hallmark of preadipocyte to adipocyte conversion. *Mech Dev* **127**, 183-202 (2010).
17. A. Polyák *et al.*, The fractalkine/Cx3CR1 system is implicated in the development of metabolic visceral adipose tissue inflammation in obesity. *Brain Behav Immun* **38**, 25-35 (2014).
18. S. M. Kabir, E. S. Lee, D. S. Son, Chemokine network during adipogenesis in 3T3-L1 cells: Differential response between growth and proinflammatory factor in preadipocytes vs. adipocytes. *Adipocyte* **3**, 97-106 (2014).
19. F. J. Ruiz-Ojeda *et al.*, Active integrins regulate white adipose tissue insulin sensitivity and brown fat thermogenesis. *Mol Metab* **45**, 101147 (2021).
20. J. Nie, A. D. Bradshaw, A. M. Delany, E. H. Sage, Inactivation of SPARC enhances high-fat diet-induced obesity in mice. *Connect Tissue Res* **52**, 99-108 (2011).
21. A. D. Bradshaw, D. C. Graves, K. Motamed, E. H. Sage, SPARC-null mice exhibit increased adiposity without significant differences in overall body weight. *Proc Natl Acad Sci U S A* **100**, 6045-6050 (2003).

22. G. Mazzolini *et al.*, SPARC expression is associated with hepatic injury in rodents and humans with non-alcoholic fatty liver disease. *Sci Rep* **8**, 725 (2018).
23. S. Mukherjee, M. J. Choi, S. W. Kim, J. W. Yun, Secreted protein acidic and rich in cysteine (SPARC) regulates thermogenesis in white and brown adipocytes. *Mol Cell Endocrinol* **506**, 110757 (2020).
24. K. El-Haschimi *et al.*, Insulin resistance and lipodystrophy in mice lacking ribosomal S6 kinase 2. *Diabetes* **52**, 1340-1346 (2003).
25. S. Al-Ghadban, I. A. Pursell, Z. T. Diaz, K. L. Herbst, B. A. Bunnell, 3D Spheroids Derived from Human Lipedema ASCs Demonstrated Similar Adipogenic Differentiation Potential and ECM Remodeling to Non-Lipedema ASCs In Vitro. *Int J Mol Sci* **21** (2020).
26. A. Bouloumié, C. Sengenès, G. Portolan, J. Galitzky, M. Lafontan, Adipocyte produces matrix metalloproteinases 2 and 9: involvement in adipose differentiation. *Diabetes* **50**, 2080-2086 (2001).
27. D. Bauters, I. Scroyen, M. Van Hul, H. R. Lijnen, Gelatinase A (MMP-2) promotes murine adipogenesis. *Biochim Biophys Acta* **1850**, 1449-1456 (2015).
28. D. B. Bosco *et al.*, A new synthetic matrix metalloproteinase inhibitor reduces human mesenchymal stem cell adipogenesis. *PLoS One* **12**, e0172925 (2017).
29. F. Tremblay *et al.*, Bidirectional modulation of adipogenesis by the secreted protein Ccdc80/DRO1/URB. *J Biol Chem* **284**, 8136-8147 (2009).
30. J. I. Grill *et al.*, Loss of DRO1/CCDC80 results in obesity and promotes adipocyte differentiation. *Mol Cell Endocrinol* **439**, 286-296 (2017).
31. C. Matthaeus *et al.*, EHD2-mediated restriction of caveolar dynamics regulates cellular fatty acid uptake. *Proc Natl Acad Sci U S A* **117**, 7471-7481 (2020).
32. B. Morén *et al.*, EHD2 regulates adipocyte function and is enriched at cell surface-associated lipid droplets in primary human adipocytes. *Mol Biol Cell* **30**, 1147-1159 (2019).
33. C. Zhao *et al.*, MAT2A promotes porcine adipogenesis by mediating H3K27me3 at Wnt10b locus and repressing Wnt/β-catenin signaling. *Biochim Biophys Acta Mol Cell Biol Lipids* **1863**, 132-142 (2018).
34. X. Wang *et al.*, Proteinase-activated receptor 2 promotes 3T3-L1 preadipocyte differentiation through activation of the PI3K/AKT signalling pathway and. *Arch Physiol Biochem* **126**, 468-475 (2020).